

Inhibition of Obtusifolin on retinal pigment epithelial cell growth under hypoxia

Li-Fei Wang¹, Zhong-Yang Yan¹, Ya-Lin Li¹, Yan-Hui Wang¹, Sheng-Juan Zhang¹, Xin Jia¹, Lu Lu², Yan-Xia Shang², Xin Wang³, Yun-Huan Li¹, Shan-Yu Li¹

¹Fundus Surgery Ward, Hebei Provincial Eye Hospital, Xingtai 054001, Hebei Province, China

²Diabetic Eye Disease Ward, Hebei Provincial Eye Hospital, Xingtai 054001, Hebei Province, China

³Corneal Disease Ward, Hebei Provincial Eye Hospital, Xingtai 054001, Hebei Province, China

Co-first authors: Li-Fei Wang and Zhong-Yang Yan

Correspondence to: Li-Fei Wang. Fundus Surgery Ward, Hebei Provincial Eye Hospital, No.399 East Quanbei Street, Qiaodong District, Xingtai 054001, Hebei Province, China. lifeiw_wanglf@163.com

Received: 2018-08-15 Accepted: 2019-06-11

DOI:10.18240/ijo.2019.10.04

Citation: Wang LF, Yan ZY, Li YL, Wang YH, Zhang SJ, Jia X, Lu L, Shang YX, Wang X, Li YH, Li SY. Inhibition of Obtusifolin on retinal pigment epithelial cell growth under hypoxia. *Int J Ophthalmol* 2019;12(10):1539-1547

INTRODUCTION

As a degenerative cause, choroidal neovascularization (CNV) is the pathological basis of various eye diseases such as age-related macular degeneration (AMD), myopic macular degeneration (PM) and central exudative chorioretinopathy (CEC)^[1-5]. The mechanism of occurrence and development of CNV is complex, the principle is not yet clear, and treatment is difficult.

Current treatments for CNV include surgery to remove or block CNV, intravitreal injections of anti-angiogenic drugs such as anti-vascular endothelial growth factor (VEGF), and using of glucocorticoids and inflammatory reactions^[6-8]. However, the efficacies of the above methods are not satisfactory, because of poor long-term efficacy, high recurrence rate, high price, and many adverse reactions^[6-8]. Although modern medicine has developed rapidly in CNV studies, the clinical efficacy of current CNV is not effective. Therefore, it is of great significance to explore new treatments.

Semen Cassiae is dry, mature seed of the leguminous plant *Cassia obtusifolia* L. or *Cassia tora* L. It is an ancient Chinese medicine that can be used as a food and medicine^[9]. The main active ingredient of cassia is Obtusifolin, which has antioxidant and nominal effects^[10]. Study has reported that the activity of ciliary lactate dehydrogenase (LDH) in obtusifolin-fed dogs and rabbits was significantly elevated^[8]. Therefore, we speculate that Obtusifolin has effects on the treatment of CNV. The generation of blood vessels refers to the process of forming a new capillary network by sprouting or intussusception after the body or tissue receiving the stimulus^[11]. Current research suggests that hypoxia is one of the most important causes of the occurrence and development of CNV and studies have confirmed that VEGF plays a key role in the formation of CNV^[12-13]. The hypoxia inducible factor-1(HIF-1)/VEGF/eNOS pathway is mainly induced by hypoxic environment,

Abstract

• **AIM:** To explore the effect of Obtusifolin on retinal pigment epithelial cell growth under hypoxia.

• **METHODS:** *In vitro* chemical hypoxia model of ARPE-19 cells was established using cobalt chloride (CoCl₂). Cell viability was tested by cell counting kit-8 (CCK-8) assay. Western blot and real-time quantitative polymerase chain reaction were applied to detect proteins and mRNAs respectively. Flow cytometry was used to examine the cell cycle. Secretion of vascular endothelial growth factor (VEGF) was tested by using enzyme linked immunosorbent assay (ELISA).

• **RESULTS:** Under the chemical hypoxia model established by CoCl₂, hypoxia inducible factor-1 α (HIF-1 α) mRNA and protein levels was up-regulated. Cell viability was increased and the proportion of S phase was higher. Obtusifolin could reduce cell viability under hypoxic conditions and arrest cells in G1 phase. Obtusifolin reduced the expression of Cyclin D1 and proliferating cell nuclear antigen (PCNA) in the hypoxic environment and increased the expression of p53 and p21. The levels of VEGF, VEGFR2 and eNOS proteins and mRNA were significantly increased under hypoxia while Obtusifolin inhibited the increasing.

• **CONCLUSION:** Obtusifolin can inhibit cell growth under hypoxic conditions and down-regulate HIF-1/VEGF/eNOS secretions in ARPE-19 cells.

• **KEYWORDS:** retinal pigment epithelial cells; Obtusifolin; vascular endothelial growth factor; hypoxia

Table 1 The sequences of primers

Primer name	Sequence (5'-3')	Product size (bp)
HIF-1 α -forward	ACCTATGACCTGCTTCCTGC	98
HIF-1 α -reverse	TTTAACTCAAGCTGCCTCGC	
Cyclin D1-forward	CTGGCCATGAACTACCTGGA	245
Cyclin D1-reverse	GTCACACTTGATCACTCTGG	
PCNA-forward	CACCTTAGCACTAGTATTCGAAGCAC	137
PCAN-reverse	CACCCGACGGCATCTTTATTAC	
p53-forward	CTGAGGTCGGCTCCGACTATACCACTATCC	360
p53-reverse	CTGATTCAGCTCTCGGAACATCTCGAAGCG	
P21-forward	AGTATGCCGTCGTCTGTTCG	229
P21-reverse	CTTGTCCTCCCTCCAGGTCA	
VEGF-forward	CTGGAGCGTGACGTTGGT	177
VEGF-reverse	TTTAACTCAAGCTGCCTCGC	
VEGFR2-forward	CCAGGCAACGTAAGTGTTGAG	243
VEGFR2-reverse	GGGACCCACGTCCTAAACAAAG	
eNOS-forward	ACCCTCACCGCTACAACATC	217
eNOS-reverse	GCTCATTCTCCAGGTGCTTC	
GAPDH-forward	CCATCTTCCAGGAGCGAGAT	222
GAPDH-reverse	TGCTGATGATCTTGAGGCTG	

activates eNOS release of NO and other factors through signal transduction, regulates cell proliferation, apoptosis, and migration^[14-15]. It is considered that VEGF-related pathways and proteins are overexpressed in ocular diseases where CNV is the pathological basis^[16-17].

This study explored the effects of Obtusifolin on cell viability and VEGF in human retinal epithelial cells under hypoxic conditions, and explored its effects on CNV.

MATERIALS AND METHODS

Cells Culture and Observation The human retinal epithelial cells line (ARPE-19) was purchased from ATCC (USA). The cells were cultured in RPMI 1640 medium containing 10% fetal bovine serum and 100 U/mL of penicillin-streptomycin mixture in an incubator at 37°C in 5% CO₂. According to different groups, the corresponding concentration (100, 200, 400 μ g/mL) of Obtusifolin was added to the culture medium and incubated at 37°C in 5% CO₂ for 24h. Obtusifolin was dissolved in DMSO and the amount of DMSO did not exceed 0.1% of the total volume of the medium. An *in vitro* chemical hypoxia model was established by adding cobalt chloride (CoCl₂; Sigma, USA) to the culture medium. Cell culture-related reagents were purchased from Gibco (USA). All cells in this experiment were within 5 passages. ARPE-19 cells morphology was observed through a light microscope (Nikon, Japan).

Cell Viability Analysis Cell counting kit-8 (CCK-8) assay was used to detect cell viability at 12, 24, and 48h after added 0, 50, 100, 150, 200 μ mol/L CoCl₂. The kit was purchased from Tongren (Japan). Diluted CCK-8 reagent were added and

cultured at 37°C in 5% CO₂ atmosphere for 4h. The absorbance of each well at 450 nm was measured using a microplate reader (ELX 800, Bio-Teck, USA), and cell viability was calculated according to the standard curve.

Real-time Quantitative Polymerase Chain Reaction

Analysis Real-time quantitative polymerase chain reaction analysis (RT-qPCR) was used to detect the mRNA expression levels of HIF-1 α , Cyclin D1, proliferating cell nuclear antigen (PCNA), p53, p21, VEGF, VEGFR2 and eNOS. The cells were triturated and lysed using Trizol (TaKaRa, Japan) at 0°C for 5min. The RNAs were extracted by CCl₄ (Aladdin, China) and dissolved in DEPC water (Sigma aliquots). RNA concentration was measured by using a UV spectrophotometer (NanoDrop One Microvolume UV-Vis spectrophotometer, Thermofisher, USA). Reverse transcription assays were performed on RNA samples using a reverse transcription kit (TaKaRa, Japan) to synthesize cDNA. Reverse transcription reaction conditions was 37°C for 15min and reverse transcriptase inactivation condition was 85°C for 15s. RT-qPCR experiments were performed with the SYBR Prellix Ex Taq™ Real-Time PCR Kit (TaKaRa, Japan). PCR was performed by activating the DNA polymerase at 95°C for 5min, followed by 40 cycles of two-step PCR (95°C for 10s and 60°C for 30s) and a final extension at 75°C for 10min and held at 4°C. DnaSe and RNase-free water were used as the templates of negative control experiences. All primers were obtained from Genewiz (Suzhou, Jiangsu China) and listed in Table 1. GAPDH was considered as an internal control. The formula 2^{- Δ ACT} was implemented to analyze the gene expression.

Western Blot Western blot was applied to detect protein expression. Cells were lysed with liquid nitrogen and blocked with RIPA (Abmole, USA), followed by 1% cleavage in PMSF and phosphatase inhibitors (Abmole, USA) and lysis for 30min at 4°C. The supernatant was collected by centrifugation at 12 000 rpm at 4°C for 15min. A standard curve was drawn using the BCA method to determine the protein concentration. A 10% SDS-PAGE gel was prepared without RNase dH₂O and used to electrophoresis. The PVDF membrane (Bio-Rad, USA) was transferred using a Trans-Blot Transfer Slot (Bio-Rad, USA) and blocked with 5% fat-free milk for 2h at room temperature. The primary antibody (anti-HIF-1 α , Abcam, ab51608, dilution: 1:800; anti-Cyclin D1, Abcam, ab134175, dilution: 1:800; anti-PCNA, ab29, Abcam, dilution: 1:700; anti-p53, Abcam, ab26, dilution: 1:600; anti-p21, Abcam, ab109520, dilution: 1:600; anti-VEGF, Merck Millipore, ABS82, dilution: 1:800; anti-VEGFR2, Abcam, ab2349, dilution: 1:600; anti-eNOS, Abcam, ab76198, dilution: 1:900) was added according to the kit instructions, shaking at room temperature for 2h, then incubated at 4°C for 12h. The secondary antibody (goat anti-mouse IgG, Abcam, ab6785, 1:8000; rabbit anti-mouse IgG, Abcam, ab99697, dilution: 1:9000; mouse anti-rabbit IgG, Invitrogen, BA1034, 1:7000; donkey anti-rabbit IgG, R&D, NL004, 1:5000; rabbit anti-human IgG, Abcam, ab6759, dilution:1:10000) was added and incubated at room temperature for 1.5h. Chemiluminescence detection was carried out use ECL reagent (Huiying, Shanghai, China).

Evaluation of Cell Cycle Cell cycle was tested by flow cytometry. The cells were collected and washed with PBS at 0°C, and then fixed with 75% ethanol at -20°C for 12h. After fixation, the cells were treated with 10 μ L of RNase A (10 mg/mL, TaKaRa, Japan) for 30min at 37°C. And then detected by flow cytometer (Becton Dickerson, SanJose, CA, USA). The flow cytometry results were processed by FlowJo V10 software (Becton, Dickinson & Company, USA).

Enzyme Linked Immunosorbent Assay The VEGF concentration of culture fluid was tested using enzyme linked immunosorbent assay (ELISA). The kits were purchased from Nanjing Kaiji Biotechnology Co., Ltd. (China). The primary antibody was added at 4°C overnight, after washing blocking solution was added at 4°C for 2h. And then the secondary antibody was added and incubated for 1h at room temperature. Horseradish peroxidase (HRP) was dropwised for 0.5h at room temperature, and tetramethylbenzidine (TMB) was added for 10min. The absorbance value was measured at 450 nm by a microplate reader (ELX 800, Bio-Teck, USA) and the concentration was calculated according to the standard curve.

Statistical Analysis All the experimental data were presented as mean \pm standard deviation (SD). Statistical analysis used

SPSS 20 (SPSS, Inc., Chicago, IL, USA). The one-way analysis of variance (ANOVA) following Turkey's multiple comparison was carried out to evaluate the differences between the experimental groups. The statistical significant was expressed as $P < 0.05$.

RESULTS

Changes of Cell Viability in Hypoxia The viable ARPE-19 macrophages were normal at 100-fold and 200-fold observations (Figure 1A). The cell viability gradually increased with the increase of CoCl₂ concentration and the passage of time. The maximal cell viability was observed in 200 μ mol/L CoCl₂ at 48h (Figure 1B). To test the successful establishment of a chemical hypoxia model, HIF-1 α mRNA and protein were detected after added CoCl₂ 24h. The expression of HIF-1 α mRNA and protein gradually increased and the maximal HIF-1 α mRNA was in 150 μ mol/L CoCl₂ (Figure 1C, 1D). This proved that the chemical hypoxia model was successfully established. The hypoxic environment has the effect of increasing the viability of human retinal epithelial cell lines. The subsequent experimental hypoxia model were established under a CoCl₂ concentration of 150 μ mol/L.

Effects of Obtusifolin on ARPE-19 Cells under Hypoxia

To study the effects of Obtusifolin on ARPE-19 cells under a hypoxic environment, cells were pretreated with 100, 200, and 400 μ g/mL Obtusifolin before adding CoCl₂. The cell viability gradually and cell count were all decreased with the increase of the concentration of Obtusifolin, and the cell viability in 400 μ g/mL concentrations was similar to that of the control group. This suggests that Obtusifolin could reduce ARPE-19 cells viability under hypoxic condition (Figure 2A, 2B).

To explore the factors that influenced the viability of ARPE-19 cells by Obtusifolin, the cell cycle was examined by using flow cytometry. Chemical hypoxia caused the ARPE-19 cells to enter the S phase to accelerate the division. Obtusifolin could restore the cell cycle under a hypoxic environment similar to the control group. This indicates that the viability and proliferative capacity of the ARPE-19 cells were inhibited in the presence of Obtusifolin (Figure 2C-2E).

Effects of Obtusifolin on Cell Cycle Associated Protein

To investigate the effects of 100, 200, 400 μ g/mL Obtusifolin on the cell cycle under hypoxic environments, the expression levels of cell cycle-associated proteins and mRNAs were determined by Western blot and RT-qPCR. When ARPE-19 cells were under hypoxic conditions, the levels of Cyclin D1 and PCNA protein and mRNA were significantly increased while the levels of p53 and p21 were decreased (Figure 3). The presence of Obtusifolin inhibited the expression of Cyclin D1 and PCNA in hypoxic conditions and up-regulated p53 and p21 levels. With the concentration of Obtusifolin increased, the effects increased (Figure 3). This suggested that hypoxia

Inhibition of Obtusifolin on RPE cells

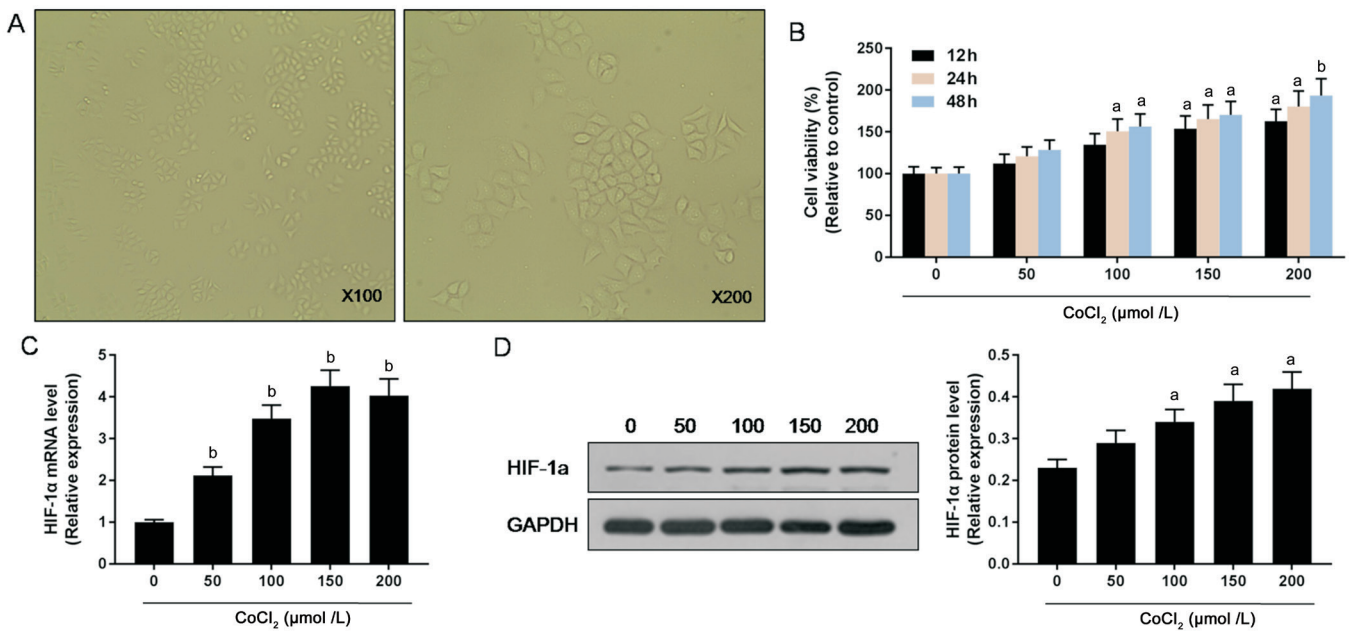


Figure 1 Effects of hypoxia on ARPE-19 cells A: The morphology of ARPE-19 cells at 100-fold and 200-fold were observed using microscope; B: The cell viability of ARPE-19 cells under different CoCl_2 concentrations at 12, 24, 48h were measured using the CCK-8 assay; C, D: Expression levels of HIF-1 α mRNA and protein under different CoCl_2 concentrations were tested by RT-qPCR and Western blot respectively. ^a $P < 0.05$, ^b $P < 0.01$ versus 0 $\mu\text{mol/L}$ CoCl_2 group.

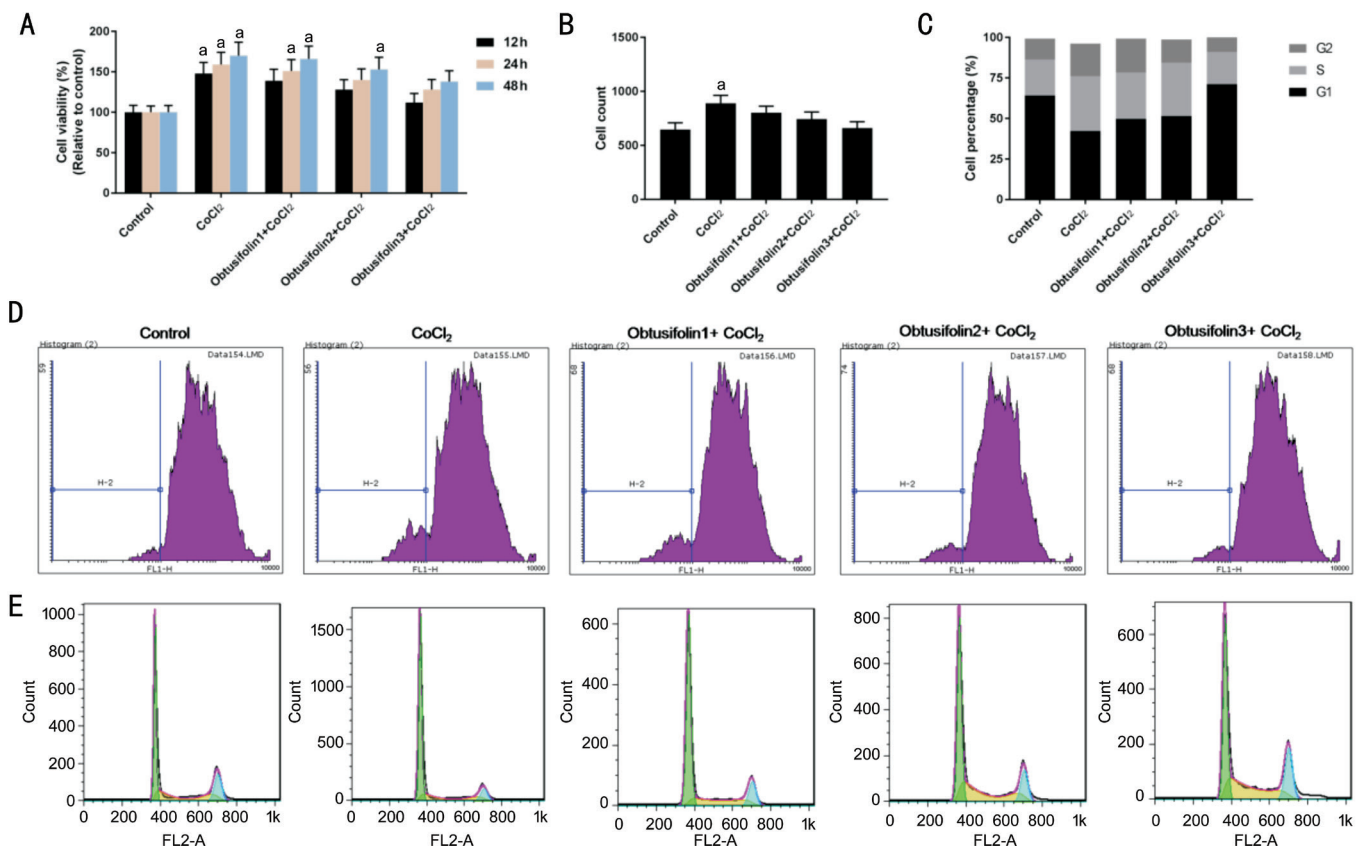


Figure 2 Effects of Obtusifolin on the cell cycle of ARPE-19 cells under hypoxia A: Cell viability under 100, 200, 400 $\mu\text{g/mL}$ Obtusifolin concentration for 24h in a hypoxic environment; B: Cell count under 100, 200, 400 $\mu\text{g/mL}$ Obtusifolin for 24h in a hypoxic environment; C-E: Flow cytometry was applied to detect the cell cycle under 100, 200, 400 $\mu\text{g/mL}$ Obtusifolin in a hypoxic environment. Obtusifolin1, Obtusifolin2, and Obtusifolin3 represent 100, 200, and 400 $\mu\text{g/mL}$ concentrations respectively. ^a $P < 0.05$ versus control group.

could promote cell proliferation and division by regulating cell cycle-associated proteins, while Obtusifolin could reduce cell

proliferation by affecting cell cycle-associated proteins and promote cells retention in the G1 phase.

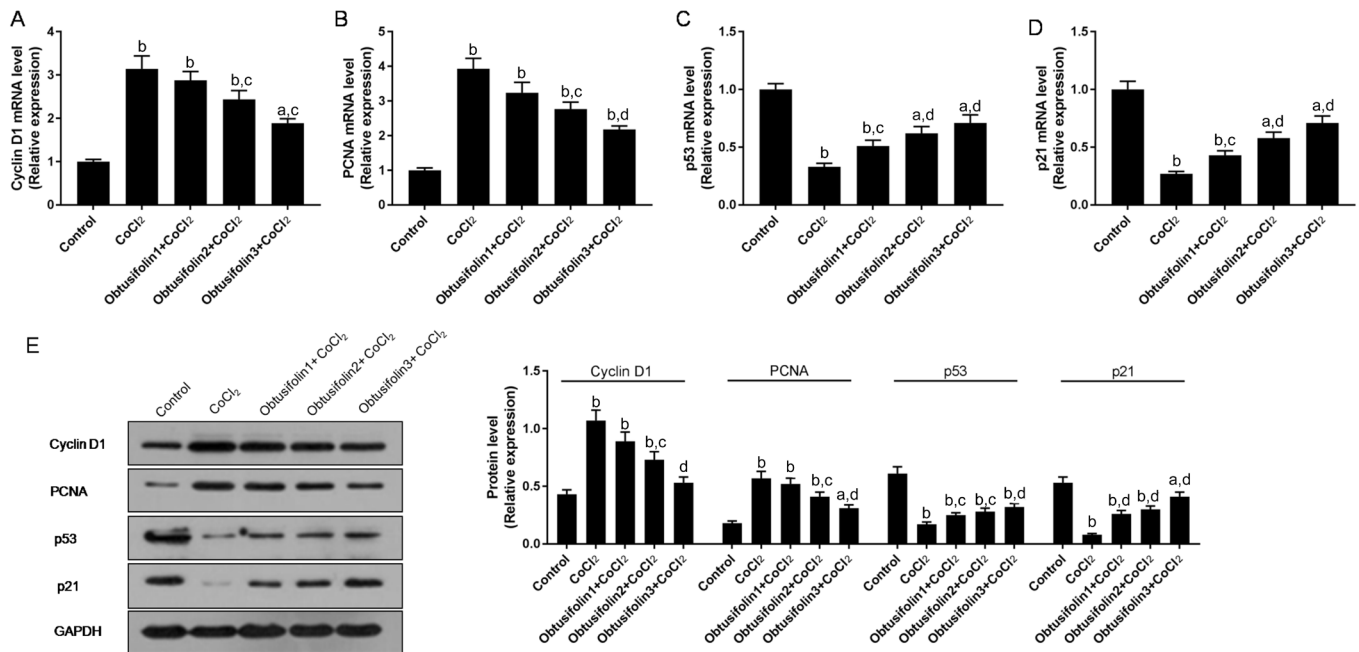


Figure 3 Effect of Obtusifolin on cell cycle associated proteins A-D: Cyclin D1, PCNA, p53 and p21 mRNAs were detected by RT-qPCR under 100, 200, 400 µg/mL Obtusifolin; E: Cyclin D1, PCNA, p53 and p21 proteins were detected using Western blot. Obtusifolin1, Obtusifolin2, and Obtusifolin3 represent 100, 200, and 400 µg/mL concentrations respectively. ^a*P*<0.05, ^b*P*<0.01 versus control group; ^c*P*<0.05, ^d*P*<0.01 versus CoCl₂ group.

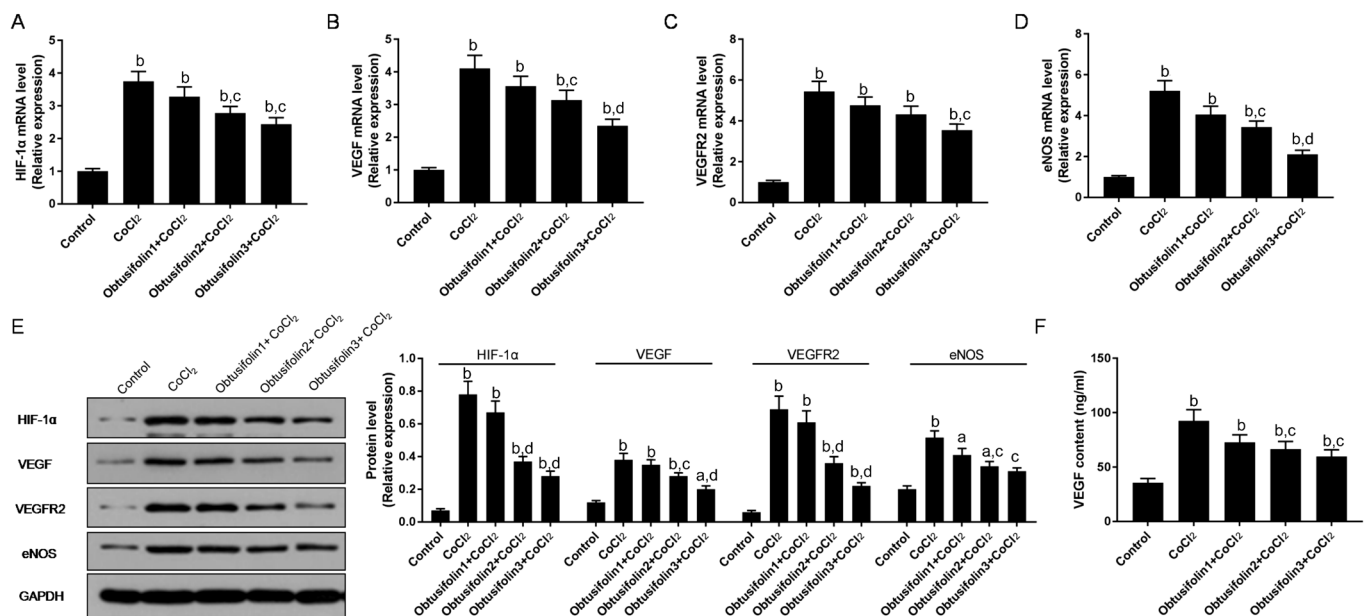


Figure 4 Effect of Obtusifolin on HIF-1, VEGF, and eNOS A-D: RT-qPCR was applied to detect HIF-1α, VEGF, VEGFR2 and eNOS mRNA expressions under 100, 200, 400 µg/mL Obtusifolin; E: Western blot was used to test HIF-1α, VEGF, VEGFR2 and eNOS protein expressions under 100, 200, 400 µg/mL Obtusifolin; F: Secretion of VEGF under 100, 200, 400 µg/mL Obtusifolin were detected by ELISA. Obtusifolin1, Obtusifolin2, and Obtusifolin3 represent 100, 200, and 400 µg/mL concentrations respectively. ^a*P*<0.05, ^b*P*<0.01 versus control group; ^c*P*<0.05, ^d*P*<0.01 versus CoCl₂ group.

Effects of Obtusifolin on HIF-1, VEGF, and eNOS To study the effects of Obtusifolin on the HIF-1, VEGF, and eNOS in the hypoxic cell model, the expression levels of the relevant mRNA and protein in the pathway were detected by RT-qPCR and Western blot respectively. When ARPE-19 cells were exposed to hypoxia, the levels of HIF-1α, VEGFR2 and eNOS proteins and

mRNA were significantly increased (Figure 4). Obtusifolin could dose-dependently down-regulate the expression of the pathway to make it close to the control group (Figure 4). The level of VEGF secreted by ARPE-19 cells was significantly elevated under the induction of hypoxia. Obtusifolin dose-dependently down-regulated VEGF secretion (Figure 4F).

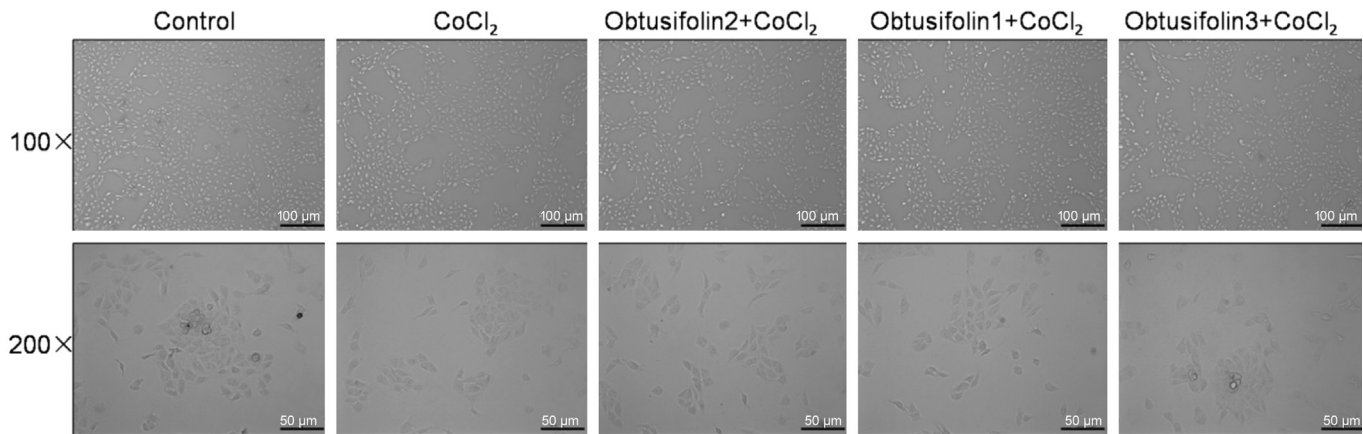


Figure 5 Effect of Obtusifolin on cell morphology The effects of 100, 200, 400 μg/mL Obtusifolin on ARPE-19 cells was observed under a microscope.

Effects of Obtusifolin on ARPE-19 Cells The effects of different concentrations of Obtusifolin on cells was observed under a microscope (Figure 5). The possible mechanism of Obtusifolin was shown in Figure 6.

DISCUSSION

The main pathological basis of angiogenesis caused by hypoxia or inflammatory cytokines is overexpression of VEGF^[18]. Angiogenesis is a complex process that involves the proliferation, migration and tube formation of vascular endothelial cells^[19-20]. CNV blood vessels mainly come from the retinal pigment epithelial cell^[18], so this study uses human retinal pigment epithelial cells line ARPE-19 cells as the research object. CoCl₂ has a low affinity with O₂ and does not have the effect of regulating O₂ concentration. However, Co²⁺ can replace the chelation of Fe²⁺ and hemoglobin, which destroys the ability of cells to sense hypoxia and thus mimic the hypoxic microenvironment^[21]. The study also finds that CoCl₂ can protect cells through anti-apoptosis pathways, and the method is simple, stable and easy to control^[22]. Therefore, CoCl₂ was used to simulate an *in vitro* chemical hypoxia microenvironment in this study. The results showed that the HIF-1α and cell viability were increased in a dose-dependent manner in the ARPE-19 cells treated with CoCl₂, demonstrating the successful establishment of an *in vitro* chemical hypoxia model.

Obtusifolin, including Emodin, Chrysophanol, Rhein, and Aloe-emodin, has a variety of biological activities, of which the eyesight is one of its most importance^[10]. The results of this study showed that Obtusifolin had the effect of reducing the cell viability of ARPE-19 cells under hypoxic conditions. Further studies have also found that Obtusifolin could promote the retention in the G1 phase and inhibit the proliferation of ARPE-19 cells. Hou *et al*^[23] found that Obtusifolin has the effect of promoting apoptosis of retinal capillary cells in diabetic retinopathy rats. And other studies suggest that for

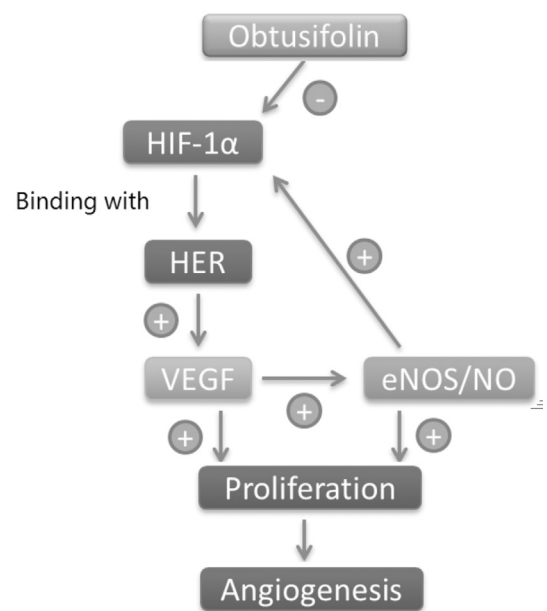


Figure 6 The possible mechanism of Obtusifolin When retinal epithelial cells are in anoxic environment, HIF-1α is overexpressed and binds to HIF-1β to form a dimer. The dimer is gradually transferred to the nucleus in combination with the hypoxia response element (HER), which promotes overexpression of the VEGF gene and promotes cell proliferation and angiogenesis. On the other hand, VEGF can regulate the level of HIF-1α by NO. Obtusifolin may inhibit cell proliferation and angiogenesis by regulating oxidative stress levels or inhibiting HIF-1α expression.

hyperlipidemic rats, Obtusifolin shows anti-oxidation and NO regulation^[24]. This showed that Obtusifolin inhibits the proliferation and differentiation of ARPE-19 cells, suggesting that it has a certain anti-angiogenic ability.

To further explore the mechanism of the effect of Obtusifolin on cell viability, we studied cell cycle-related proteins by Western blot and RT-qPCR. The results showed that Obtusifolin could dose-dependently down-regulate Cyclin D1 and PCNA in ARPE-19 cells under hypoxia and up-regulate p53 and p21 levels. Cyclin D1 is one of the most

important proteins that regulate cell cycle, it can bind and activate the unique cyclin-dependent kinase CDK4 during G1, promoting cell cycle progression from G1 to S, thereby promoting cell proliferation^[25]. PCNA is involved in cellular DNA synthesis. PCNA was not expressed in G0-G1 phase cells, but it was significantly increased in the late G1 phase, and PCNA was a sensitive indicator of cell cycle response^[26]. As a tumor suppressor gene, p53 has the effect of inhibiting cell proliferation by tissue cycle^[27]. The p21 gene is a member of the Clp family and it is a cyclin-dependent kinase inhibitor downstream of the p53 gene^[28]. P21 can together with p53 constitute the cell cycle G1 checkpoint^[29]. The results of this study suggest that Obtusifolin could inhibit cell proliferation by up-regulating tumor suppressor genes and down-regulating cyclin proteins.

The proliferation of cells is affected by a variety of cellular pathways. For the proliferation of retinal pigment epithelial cells and the formation of blood vessels, the largest influencing factor is the hypoxic microenvironment, and overexpression of VEGF is the main cause of vascular proliferation^[30-31]. HIF-1 is a key upstream transcription factor in angiogenesis signaling pathway, HIF-1 can be divided into HIF-1 α and HIF-1 β ^[32]. When the body is under hypoxia, it will induce high expression of HIF-1 α , and it will up-regulate the expression of VEGF after binding with VEGF gene through hypoxia response element (HER)^[33]. As a key protein in the pathway, VEGF mainly promotes the release of eNOS and NO through the activation of PI3K/Akt, MAPK and JAK/STAT pathway^[34-36]. NO is an essential angiogenesis profile factor^[37-38]. On the other hand, PI3K/Akt and other pathways also have the effect of promoting cell proliferation and anti-apoptosis^[39-40]. The results of this study indicated that the hypoxic microenvironment could promote the expression and secretion of VEGF by increasing the expression of HIF-1 α , and promote the expression of VEGFR2 and eNOS. Obtusifolin could down-regulate the HIF-1 α , decrease the expression and secretion of VEGF. Previous studies have shown that improving the hypoxic state can play an anti-angiogenic role by inhibiting VEGF^[41-42]. Studies have also found that inhibiting the expression and secretion of VEGF can exert an anti-angiogenic effect by inhibiting the expression of NO^[43]. Tang and Zhong's study^[44] shows that Obtusifolin can regulate oxidative stress levels associated with obesity and diabetes. Obtusifolin regulates the levels of SOD and MDA to down-regulate oxidative stress levels. In addition, the study also finds that Obtusifolin regulates the level of NO^[44]. Study has also shown that Obtusifolin could reduce the level of inflammatory factors by inhibiting nuclear factor-kappa B, which might also be related to angiogenesis^[45]. This study first discovered that Obtusifolin could inhibit angiogenesis by inhibiting signal transduction by downregulating HIF-1 α and

reducing VEGF expression. In addition, Obtusifolin may also inhibit VEGF expression and may also inhibit cell proliferation by inhibiting VEGF related pathways and further studies are needed. Hypoxia could promote angiogenesis possibly by inducing the expression of VEGF, while Obtusifolin could inhibit the expression and secretion of VEGF by down-regulating HIF-1 α , thereby reducing the inhibition of angiogenesis by eNOS.

ACKNOWLEDGEMENTS

Authors' contributions: Substantial contributions to conception and design: Wang LF, Yan ZY; Data acquisition: Li YL, Wang YH; Data analysis and interpretation: Zhang SJ, Jia X; Drafting the article or critically revising it for important intellectual content: Lu L, Shang YX; Final approval of the version to be published: Wang X, Li YH; Agreement to be accountable for all aspects of the work in ensuring that questions related to the accuracy or integrity of the work are appropriately investigated and resolved: Li SY; All authors read and approved the final manuscript.

Conflicts of Interest: Wang LF, None; Yan ZY, None; Li YL, None; Wang YH, None; Zhang SJ, None; Jia X, None; Lu L, None; Shang YX, None; Wang X, None; Li YH, None; Li SY, None.

REFERENCES

- 1 Jia YL, Bailey ST, Wilson DJ, Tan O, Klein ML, Flaxel CJ, Potsaid B, Liu JJ, Lu CD, Kraus MF, Fujimoto JG, Huang D. Quantitative optical coherence tomography angiography of choroidal neovascularization in age-related macular degeneration. *Ophthalmology* 2014;121(7):1435-1444.
- 2 Amalric P. Choroidal neovascularization. *Annee Ther Clin Ophthalmol* 1979;30:111-128.
- 3 Freund KB, Yannuzzi LA, Sorenson JA. Age-related macular degeneration and choroidal neovascularization. *Am J Ophthalmol* 1993;115(6):786-791.
- 4 Inhoffen W, Ziemssen F. Morphological features of myopic choroidal neovascularization: differences to neovascular age-related macular degeneration. *Ophthalmologie* 2012;109(8):749-757.
- 5 Weng S, Mao L, Yu S, Gong Y, Cheng L, Chen X. Detection of choroidal neovascularization in central serous chorioretinopathy using optical coherence tomographic angiography. *Ophthalmologica* 2016;236(2):114-121.
- 6 Wong TY, Ferreira A, Hughes R, Carter G, Mitchell P. Epidemiology and disease burden of pathologic myopia and myopic choroidal neovascularization: an evidence-based systematic review. *Am J Ophthalmol* 2014;157(1):9-25.e12.
- 7 Farinha CL, Baltar AS, Nunes SG, Figueira JP, Pires IA, Cachulo ML, Silva RM. Progression of myopic maculopathy after treatment of choroidal neovascularization. *Ophthalmologica* 2014;231(4):211-220.
- 8 Ferris FL 3rd, Wilkinson CP, Bird A, Chakravarthy U, Chew E, Csaky K, Sarda SR; Beckman Initiative for Macular Research Classification Committee. Clinical classification of age-related macular degeneration. *Ophthalmology* 2013;120(4):844-851.

- 9 Zhang WD, Wang Y, Wang Q, Yang WJ, Gu Y, Wang R, Song XM, Wang XJ. Quality evaluation of Semen Cassiae (*Cassia obtusifolia* L.) by using ultra-high performance liquid chromatography coupled with mass spectrometry. *J Sep Sci* 2012;35(16):2054-2062.
- 10 Liu C, Liu Q, Sun J, Jiang B, Yan J. Extraction of water-soluble polysaccharide and the antioxidant activity from Semen cassiae. *J Food Drug Anal* 2014;22(4):492-499.
- 11 Ackermann M, Houdek JP, Gibney BC, Ysasi A, Wagner W, Belle J, Schittny JC, Enzmann F, Tsuda A, Mentzer SJ, Konerding MA. Sprouting and intussusceptive angiogenesis in postpneumonectomy lung growth: mechanisms of alveolar neovascularization. *Angiogenesis* 2014;17(3):541-551.
- 12 Shweiki D, Itin A, Soffer D, Keshet E. Vascular endothelial growth factor induced by hypoxia may mediate hypoxia-initiated angiogenesis. *Nature* 1992;359(6398):843-845.
- 13 Thom R, Rowe GC, Jang C, Safdar A, Arany Z. Hypoxic induction of vascular endothelial growth factor (VEGF) and angiogenesis in muscle by truncated peroxisome proliferator-activated receptor γ coactivator (PGC)-1 α . *J Biol Chem* 2014;289(13):8810-8817.
- 14 Tang X, Zhang Q, Shi S, Yen Y, Li X, Zhang Y, Zhou K, Le AD. Bisphosphonates suppress insulin-like growth factor 1-induced angiogenesis via the HIF-1 α /VEGF signaling pathways in human breast cancer cells. *Int J Cancer* 2010;126(1):90-103.
- 15 Carbajo-Pescador S, Ordoñez R, Benet M, Jover R, García-Palomo A, Mauriz L, González-Gallego J. Inhibition of VEGF expression through blockade of Hif1 α and STAT3 signalling mediates the anti-angiogenic effect of melatonin in HepG2 liver cancer cells. *Br J Cancer* 2013;109(1):83-91.
- 16 Rakic JM, Lambert V, Devy L, Lutun A, Carmeliet P, Claes C, Nguyen L, Foidart JM, Noël A, Munaut C. Placental growth factor, a member of the VEGF family, contributes to the development of choroidal neovascularization. *Invest Ophthalmol Vis Sci* 2003;44(7):3186-3193.
- 17 Krause TA, Alex AF, Engel DR, Kurts C, Eter N. VEGF-production by CCR2-dependent macrophages contributes to laser-induced choroidal neovascularization. *PLoS One* 2014;9(4):e94313.
- 18 Croci DO, Cerliani JP, Dalotto-Moreno T, Méndez-Huergo SP, Mascanfroni ID, Dergan-Dylon S, Toscano MA, Caramelo JJ, García-Vallejo JJ, Ouyang J, Mesri EA, Junntila MR, Bais C, Shipp MA, Salatino M, Rabinovich GA. Glycosylation-dependent lectin-receptor interactions preserve angiogenesis in anti-VEGF refractory tumors. *Cell* 2014;156(4):744-758.
- 19 Puche N, Glacet A, Mimoun G, Zourhani A, Coscas G, Soubrane G. Intravitreal ranibizumab for macular oedema secondary to retinal vein occlusion: a retrospective study of 34 eyes. *Acta Ophthalmol* 2012;90(4):357-361.
- 20 Wilson BD. Netrins promote developmental and therapeutic angiogenesis. *Science* 2006;313(5787):640-644.
- 21 Ardyanto T, Osaki M, Tokuyasu N, Nagahama Y, Ito H. CoCl₂-induced HIF-1 α expression correlates with proliferation and apoptosis in MKN-1 cells: A possible role for the PI₃K/Akt pathway. *Int J Oncol* 2006;29(3):549-555.
- 22 Zhong X, Lin R, Li Z, Mao J, Chen L. Effects of Salidroside on cobalt chloride-induced hypoxia damage and mTOR signaling repression in PC12 cells. *Biol Pharm Bull* 2014;37(7):1199-1206.
- 23 Hou B, He S, Gong Y, Li Z. Effect of obtusifolin administration on retinal capillary cell death and the development of retinopathy in diabetic rats. *Cell Biochem Biophys* 2014;70(3):1655-1661.
- 24 Zhuang SY, Wu ML, Wei PJ, Cao ZP, Xiao P, Li CH. Changes in plasma lipid levels and antioxidant activities in rats after supplementation of obtusifolin. *Planta Med* 2016;82(6):539-543.
- 25 Baldin V, Lukas J, Marcote MJ, Pagano M, Draetta G. Cyclin D1 is a nuclear protein required for cell cycle progression in G1. *Genes Dev* 1993;7(5):812-821.
- 26 Strzalka W, Ziemienowicz A. Proliferating cell nuclear antigen (PCNA): a key factor in DNA replication and cell cycle regulation. *Ann Bot* 2011;107(7):1127-1140.
- 27 Matas D, Sigal A, Stambolsky P, Milyavsky M, Weisz L, Schwartz D, Goldfinger N, Rotter V. Integrity of the N-terminal transcription domain of p53 is required for mutant p53 interference with drug-induced apoptosis. *EMBO J* 2001;20(15):4163-4172.
- 28 Yoon MK, Mitrea DM, Ou L, Kriwacki RW. Cell cycle regulation by the intrinsically disordered proteins p21 and p27. *Biochem Soc Trans* 2012;40(5):981-988.
- 29 Wulf GM, Liou YC, Ryo A, Lee SW, Lu KP. Role of Pin1 in the regulation of p53 stability and p21 transactivation, and cell cycle checkpoints in response to DNA damage. *J Biol Chem* 2002;277(50):47976-47979.
- 30 Vadlapatla RK, Vadlapudi AD, Pal D, Mukherji M, Mitra AK. Ritonavir inhibits HIF-1 α -mediated VEGF expression in retinal pigment epithelial cells *in vitro*. *Eye (Lond)* 2014;28(1):93-101.
- 31 Liu NN, Zhao N, Cai N. Suppression of the proliferation of hypoxia-Induced retinal pigment epithelial cell by rapamycin through the /mTOR/HIF-1 α /VEGF/ signaling. *IUBMB Life* 2015;67(6):446-452.
- 32 Semenza GL. HIF-1 mediates metabolic responses to intratumoral hypoxia and oncogenic mutations. *J Clin Invest* 2013;123(9):3664-3671.
- 33 Park H, Lee DS, Yim MJ, Choi YH, Park S, Seo SK, Choi JS, Jang WH, Yea SS, Park WS, Lee CM, Jung WK, Choi IW. 3, 3'-Diindolylmethane inhibits VEGF expression through the HIF-1 α and NF- κ B pathways in human retinal pigment epithelial cells under chemical hypoxic conditions. *Int J Mol Med* 2015;36(1):301-308.
- 34 Yang XM, Wang YS, Zhang J, Li Y, Xu JF, Zhu J, Zhao W, Chu DK, Wiedemann P. Role of PI₃K/Akt and MEK/ERK in mediating hypoxia-induced expression of HIF-1 α and VEGF in laser-induced rat choroidal neovascularization. *Invest Ophthalmol Vis Sci* 2009;50(4):1873-1879.
- 35 Zeng D, Wang J, Kong P, Chang C, Li J, Li J. Ginsenoside Rg3 inhibits HIF-1 α and VEGF expression in patient with acute leukemia via inhibiting the activation of PI3K/Akt and ERK1/2 pathways. *Int J Clin Exp Pathol* 2014;7(5):2172-2178.
- 36 Wen Z, Huang C, Xu Y, Xiao Y, Tang L, Dai J, Sun H, Chen B, Zhou M. α -Solanine inhibits vascular endothelial growth factor expression by

- down-regulating the ERK1/2-HIF-1 α and STAT3 signaling pathways. *Eur J Pharmacol* 2016;771:93-98.
- 37 Näslund I, Norrby K. NO and de novo mammalian angiogenesis: further evidence that NO inhibits bFGF-induced angiogenesis while not influencing VEGF165-induced angiogenesis. *APMIS* 2000;108(1): 29-37.
- 38 Xia P, Chen HY, Chen SF, Wang L, Strappe PM, Yang HL, Zhou CH, Zhang X, Zhang YX, Ma LL, Wang LX. The stimulatory effects of eNOS/F92A-Cav1 on NO production and angiogenesis in BMSCs. *Biomedecine Pharmacother* 2016;77:7-13.
- 39 Gu YJ, Sun WY, Zhang S, Li XR, Wei W. Targeted blockade of JAK/STAT3 signaling inhibits proliferation, migration and collagen production as well as inducing the apoptosis of hepatic stellate cells. *Int J Mol Med* 2016;38(3):903-911.
- 40 Sun Y, Liu WZ, Liu T, Feng X, Yang N, Zhou HF. Signaling pathway of MAPK/ERK in cell proliferation, differentiation, migration, senescence and apoptosis. *J Recept Signal Transduct Res* 2015;35(6):600-604.
- 41 Bhattacharya D, Singh MK, Chaudhuri S, Acharya S, Basu AK, Chaudhuri S. T11TS impedes glioma angiogenesis by inhibiting VEGF signaling and pro-survival PI3K/Akt/eNOS pathway with concomitant upregulation of PTEN in brain endothelial cells. *J Neurooncol* 2013;113(1):13-25.
- 42 Corpechot C, Barbu V, Wendum D, Kinnman N, Rey C, Poupon R, Housset C, Rosmorduc O. Hypoxia-induced VEGF and collagen I expressions are associated with angiogenesis and fibrogenesis in experimental cirrhosis. *Hepatology* 2002;35(5):1010-1021.
- 43 Iyer AK, Ramesh V, Castro CA, Kaushik V, Kulkarni YM, Wright CA, Venkatadri R, Rojanasakul Y, Azad N. Nitric oxide mediates bleomycin-induced angiogenesis and pulmonary fibrosis via regulation of VEGF. *J Cell Biochem* 2015;116(11):2484-2493.
- 44 Tang Y, Zhong Z. Obtusifolin treatment improves hyperlipidemia and hyperglycemia: possible mechanism involving oxidative stress. *Cell Biochem Biophys* 2014;70(3):1751-1757.
- 45 He ZW, Wei W, Li SP, Ling Q, Liao KJ, Wang X. Anti-allodynic effects of obtusifolin and gluco-obtusifolin against inflammatory and neuropathic pain. *Biol Pharm Bull* 2014;37(10):1606-1616.